

3-19-2014

Experimental Study of Soil Water Migration in Freezing Process

Xuesong Mao
Chang'an University

Carol J. Miller
Wayne State University, ab1421@wayne.edu

Zhongjie Hou
Chang'an University

Abdul Khandker
Wayne State University

Recommended Citation

Mao, Xuesong; Miller, Carol J.; Hou, Zhongjie; and Khandker, Abdul, "Experimental Study of Soil Water Migration in Freezing Process" (2014). *Civil and Environmental Engineering Faculty Research Publications*. 34.
https://digitalcommons.wayne.edu/ce_eng_frp/34

This Article is brought to you for free and open access by the Civil and Environmental Engineering at DigitalCommons@WayneState. It has been accepted for inclusion in Civil and Environmental Engineering Faculty Research Publications by an authorized administrator of DigitalCommons@WayneState.



Geotechnical Testing Journal

Xuesong Mao,^{1,2} Carol Miller,² Zhongjie Hou,¹ Abdul Khandker,² and Xuan Xiao¹

DOI: 10.1520/GTJ20130119

Experimental Study of Soil Water Migration in Freezing Process

VOL. 37 / NO. 3 / MAY 2014



Xuesong Mao,^{1,2} Carol Miller,² Zhongjie Hou,¹ Abdul Khandker,² and Xuan Xiao¹

Experimental Study of Soil Water Migration in Freezing Process

Reference

Mao, Xuesong, Miller, Carol, Hou, Zhongjie, Khandker, Abdul, and Xiao, Xuan, "Experimental Study of Soil Water Migration in Freezing Process," *Geotechnical Testing Journal*, Vol. 37, No. 3, 2014, pp. 1-11, doi:10.1520/GTJ20130119. ISSN 0149-6115

ABSTRACT

Soil water migration is a significant factor in the development of subgrade ice layers in permafrost areas. The prediction of moisture inflow to the freezing zone is an important element in the design and analysis of robust highway subgrade in permafrost regions. In order to better understand moisture inflow to the freezing zone, we designed an experimental investigation to monitor the variation of water content and temperature in freezing soil. Identical experiments were conducted using three different soil types: clay, silt, and fine sand. Moisture was supplied from the sample base while the column was maintained at a constant nonfreezing temperature and moisture equilibration was achieved. A temperature gradient was then applied to the sample via the application of a subfreezing temperature at the column surface. The changes in the temperature and water content of the sample were measured at regular time intervals. Based on the freezing rate, the freezing process can be classified into three stages: the *quick frost* stage, the *transition frost* stage, and the *stable frost* stage. During the freezing process, the inflow rates increased as the thickness of the ice lens increased. When the maximum rate was reached, the final (maximum) thickness of the ice lens was attained. Subsequently, the water inflow rates decreased. All of the water supplied from the bottom of the sample flowed into the frost section during the freezing process, with the moisture contents in the lower portion remaining relatively unchanged. The segregation potential changed with the freezing rate and soil type. This paper proposes the concept of "generalized segregation potential" to extend the traditional segregation potential concept. The use of this new concept with an existing moisture inflow prediction model provided excellent correspondence to measured inflow rates for all three study soils in the early and late stages of the test but overpredicted the inflow rates in the mid-range of the test.

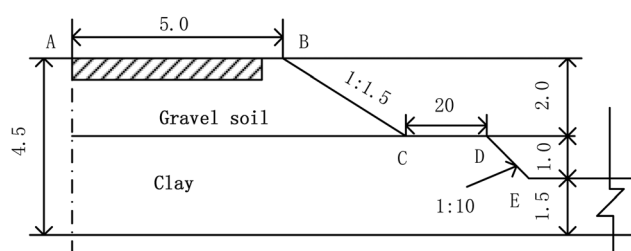
Keywords

moisture migration, freezing rate, temperature gradient, generalized segregation potential, moisture inflow

Manuscript received July 12, 2013; accepted for publication January 16, 2014; published online March 19, 2014.

¹ School of Highway, Chang'an Univ., Xi'an, 710064, China

² Dept. of Civil and Environmental Engineering, Wayne State Univ., Detroit, MI 48202, United States of America

FIG. 1 Cross-sectional profile of highway at K3020 + 200 (in meters).

Introduction

Longitudinal cracks that form due to the differential heave/settlement of foundation soils during freeze/thaw cycles are the primary cause of highway pavement damage in permafrost regions (Dou et al. 2002; Liu et al. 2002; Pei et al. 2006; Chou et al. 2008; Wen et al. 2009; Mao et al. 2010; Jin et al. 2012). In order to further understand the causes and magnitude of freeze/thaw damage, a typical highway section (K3020 + 200) was excavated at the Hoh Xil pass of Qinghai to Tibet. A 20-m longitudinal crack was observed along the shoulder of the highway. A cross-sectional profile of the highway is presented in Fig. 1. Details of the excavation site are shown in Fig. 2.

Visual observations of the excavation [Figs. 2(b) and 2(c)] confirmed that the ice lens formation and subsequent thaw were the primary cause of the highway damage. An understanding of the phenomena of ice lens formation is critical to the design of more robust highway systems in permafrost and seasonal-frost regions. Ice lens formation is dependent on water availability. Therefore, accurate prediction of highway damage due to freeze requires the capability to model moisture movement to the freezing zone and the growth of the ice lens.

When the air temperature at the soil surface is below 0°C, water at the soil surface and in the soil pores begins to freeze, causing the upward migration of soil moisture. Not all of the factors causing moisture migration toward frozen soil are fully understood. Many theories have been advanced to explain the moisture migration. Mathematical models simulating heat and

moisture movement in freezing soils have been reported by Harlan (1973), Taylor and Luthin (1978), Miao et al. (1999), Wang et al. (2004), Lei et al. (1988), and Xu et al. (2001). Frost heave studies (Tezera 2012; Bronfenbrener and Bronfenbrener 2010; Azmatch et al. 2011, 2008; Arenson et al. 2008; Zhang et al. 2004; Konrad and Duquenois 1993) indicate that soil cracks in the frozen fringe are due to ice lens formation. Cheng (1981) studied the unidirectional aggregation effect of unfrozen water under the seasonal freeze/thaw layer. The formation of the ice lens is one of the results of moisture migration in freezing soil. Konrad and Morgenstern (1981) showed that when a soil sample freezes under different cold-side step temperatures but the same warm-side temperature, at the formation of the ice lens the water intake flux is proportional to the temperature gradient in the frozen fringe. In fact, there are many factors that affect the water inflow during the freezing process. In this study an experimental setup allowed the simultaneous measurement of moisture and temperature during the application of a sub-freezing boundary condition. Information obtained from the experiment allows the improvement of the model of moisture migration in freezing conditions.

Experimental Design

EXPERIMENTAL APPARATUS

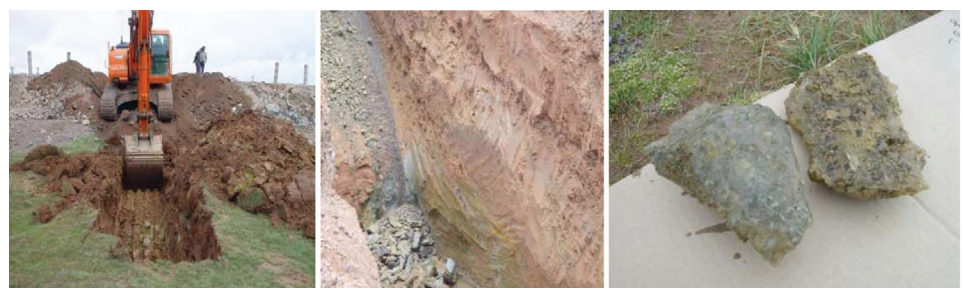
The experimental apparatus included a refrigeration unit, a water supply unit, a test chamber, temperature sensors, moisture sensors, a temperature acquisition instrument, and a moisture acquisition instrument. A schematic of the testing apparatus is shown in Fig. 3.

The refrigeration unit included a cold bath and connecting tubes that controlled the temperature at the upper boundary of the soil column. The soil was frozen from top to bottom. The control range of the refrigeration unit was from -30°C to 20°C.

The test chamber included a poly(methyl methacrylate) cylinder (65 cm in height and 20 cm in diameter), supports, and a top plate. There were a total of 12 temperature sensors and 12 moisture sensors. The precision of the temperature and

FIG. 2

View of the excavation and ice lens.



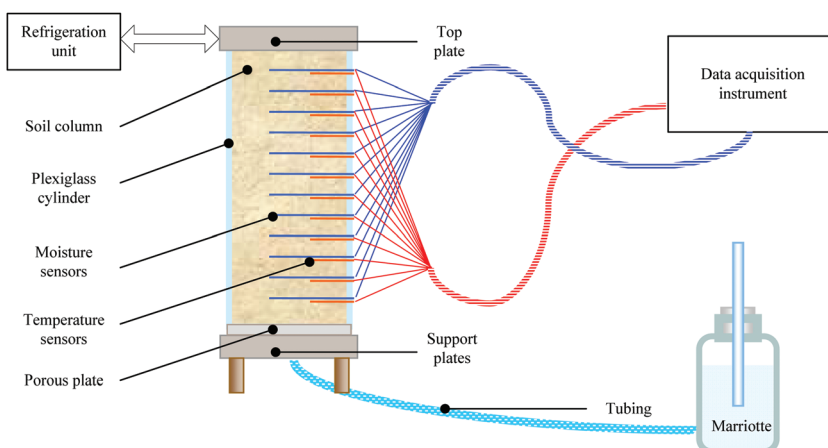
a) Excavating

b) The section

c) The ice lens

FIG. 3

Schematic of the testing apparatus.



moisture sensors was $\pm 0.1^\circ\text{C}$ and $\pm 0.1\%$, respectively. Time domain reflectometry (TDR) was used to monitor moisture changes, and temperatures were monitored using Pt 100 thermistors.

The water supply unit included a porous plate, a water supply tube, and a Mariotte bottle. The Mariotte bottle provided the moisture source, controlled the water supply level, and eliminated any effects of elevated water pressure on the bottom of the column.

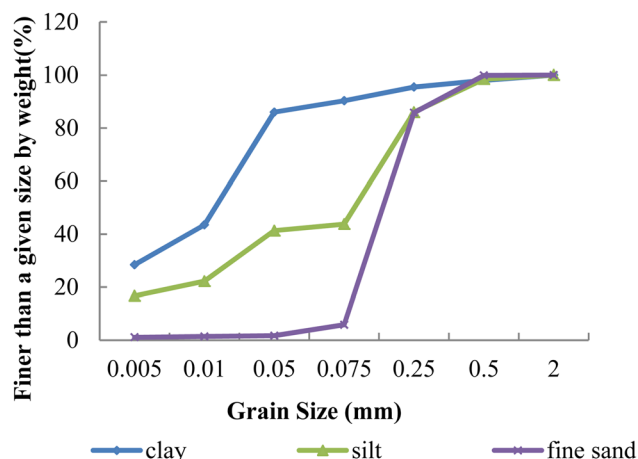
SOILS

Three types of soil were used in this study. As classified according to JTJE 40-2007, these soils were fine sand, clay, and silt. The grain size distribution of each is shown in Fig. 4. A summary of the physical properties of the soils is provided in Table 1.

PROCEDURE

The initial task involved preparation of the soil column. The soil added to the column was compacted at the optimum moisture content, yielding the maximum dry density as shown in Table 1. The moisture and temperature sensors were placed at 5-cm intervals during the compaction process.

FIG. 4 Grain size distribution of study soils.



In the subsurface, moisture migration is controlled by gradients in total energy. The total energy includes gravitational, pressure, and thermal components (the kinetic energy component is generally assumed negligible in subsurface flows). However, in regions of relatively uniform subsurface temperature, the thermal component of the energy gradient is negligible and the subsurface moisture migration is dominated by the gradient of the combined gravitational and pressure components.

In order for the effect of temperature gradients on moisture movement to be isolated, the soil moisture must initially be at an equilibrium energy state. In this condition, there is no moisture migration. Thus, the experiment proceeded in two steps. In the first step, water was supplied from the column base using a Mariotte bottle while the system was maintained at a uniform temperature (room temperature, approximately 20°C). During this step, water migration occurred as a result of gradients in energy (pressure and gravity components). Changes in soil moisture content were monitored using TDR during the isothermal migration. The cumulative water input was monitored using a precision electronic autobalance. Migration continued until equilibration was achieved throughout the column. Equilibration was assumed to have occurred when the water content measured via TDR changed by less than $\pm 0.1\%$ and the water input changed by less than $\pm 0.1\text{g}$ in a 24-h period. At this point, water inflow to the column was assumed negligible. The soil moisture values during this equilibration process are shown in Fig. 5.

TABLE 1 Summary of physical properties of the soils.

Soil	Liquid Limit $W_L, \%$	Plastic Limit $W_P, \%$	Plasticity Index I_p	Optimum Moisture Content, %	Maximum Dry Density, g/cm^3
Clay	28.8	17.4	11.4	19.1	1.96
Silt	17.8	11.4	6.4	18.4	1.90
Fine sand				8.2	1.70

Following equilibration of the soil column in step one (above), the column was wrapped with insulation foam. The second step commenced with application of a subfreezing temperature at the top of the soil column. The modified thermal boundary condition disturbed the energy equilibrium and moisture migration was initiated in response to the thermal gradient. As in step one, the water was supplied from the base of the column using the Mariotte bottle. The moisture and temperature throughout the column were monitored using TDR and thermistors, respectively. The total water supplied from the base was monitored gravimetrically, as in step one.

Experimental Data Analysis

TEMPERATURE VARIATION WITHIN THE SAMPLE

The temperature profile variation with time during step two of the experiment is provided in Fig. 6 for each of the three soil types.

At the beginning of the second step (corresponding to 0 h), the temperature was uniform throughout the column. Upon application of the subfreezing temperature from above, a frozen soil layer began to develop and the depth of the frozen soil zone increased with time. During the early periods of this step of the experiment, the temperature gradient was very steep in the upper portions of the column, but relatively uniform at lower elevations.

The temperature gradient was always larger in the upper frozen section than in the lower unfrozen section. At any given height, the temperature decreased with time and reached 0°C, which was the interface between frozen and unfrozen soil. As the depth of the frozen section increased, the average temperature gradient of the frozen section decreased significantly, but the average temperature gradient of the unfrozen section exhibited little change.

The variation in the temperature gradient was attributed to the difference in the water content and thermal properties along the length of the column. Greater moisture contents occurred at

FIG. 5

Temporal changes in liquid water content as measured via TDR.

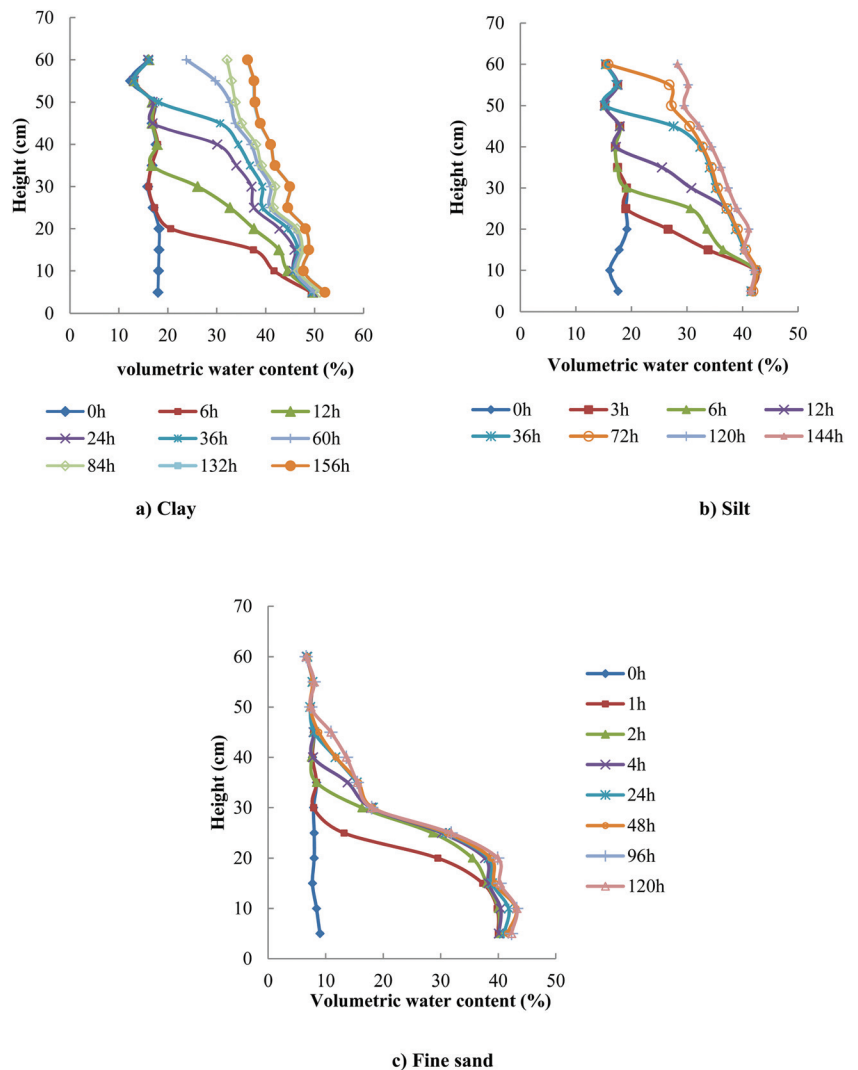
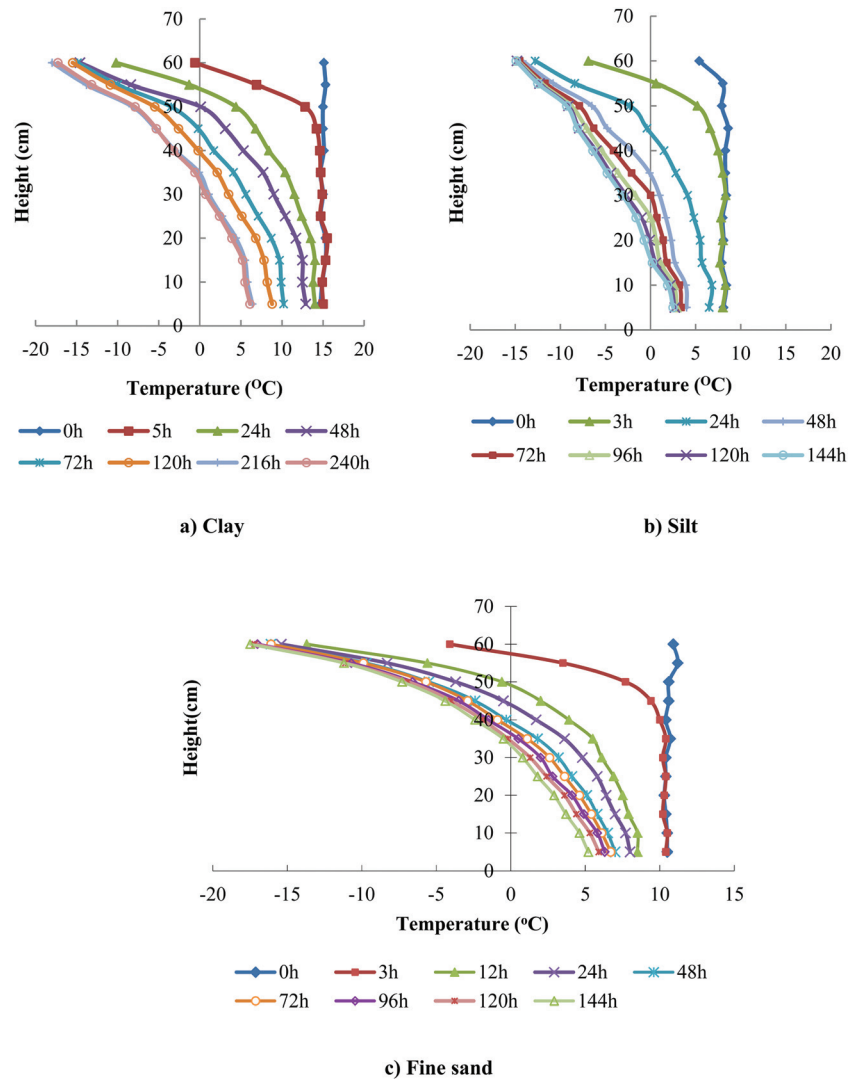


FIG. 6

Time variant curves of the internal temperature of the sample during freezing.



the base of the column, close to the water source. The thermal conductivity and specific heat capacity are dependent on the moisture content and exhibit significant differences between frozen and unfrozen sections (Xu 1981).

For similar conditions, increasing moisture contents lead to increases in specific heat capacity, resulting in greater resistance to temperature change or reduced rates of temperature change in zones of greater moisture content. Furthermore, the thermal conductivity of frozen soil exceeds that of unfrozen layers, whereas the specific heat capacity of the frozen layer is smaller than that of the unfrozen layer. All these conditions result in more rapid temperature changes in the frozen layer and explain the temperature profiles in Fig. 6.

FREEZING RATE AND PROGRESSION OF FROZEN FRONT

The advancement of the frozen soil moisture front and the variation in the freezing rate are presented in Fig. 7. The term “freezing rate” is used to describe the speed with which the

frozen front advances (in centimeters per second). In subsequent equations, the freezing rate is denoted by F . The graphs in Fig. 7 suggest that the freezing process can be divided into three characteristic stages: (I) the *quick frost stage*, (II) the *transition frost stage*, and (III) the *stable frost stage*.

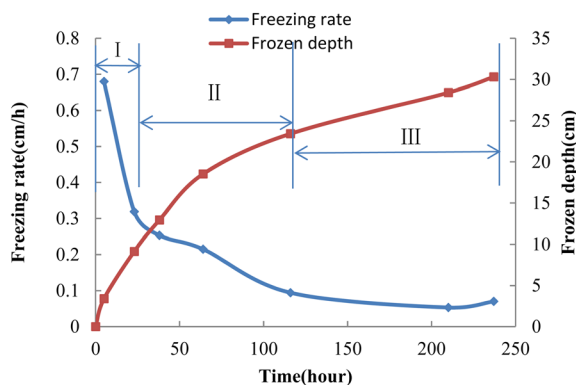
In the quick frost stage, the freezing rate was unstable, the temperature reduction was very fast, and the freezing depth increased at a fast pace. In the transition frost stage, the freezing rate was more stable, the temperature reduction was slower, and the freezing depth increased at a slower pace than in the quick frost section. In the stable frost stage, the freezing rate changed little, and the freezing depth increased very slowly. There were significant differences in moisture migration in the three stages of the freezing process, as described subsequently.

THE MOISTURE DISTRIBUTION IN DIFFERENT STAGES

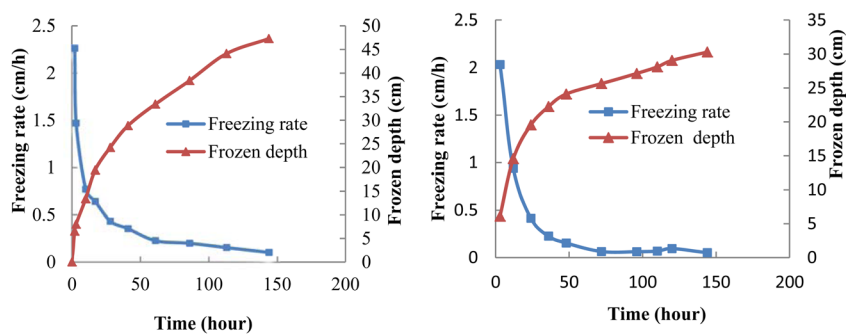
The variation of the moisture content with height is presented in Fig. 8 for a range of observation times. During the freezing

FIG. 7

Variation of the frozen depth and the freezing rate with time.



a) Clay (I quick frost stage, II transition frost stage, and III stable frost stage)



b) Silt

c) Fine sand

process, the water content changed little within the unfrozen section. For example, the bottom portion of each of the soil columns retained a relatively uniform moisture content, with only the thickness of the uniform zone changing with soil type. For example, the thickness was 30 cm, 15 cm, and 30 cm for the clay, silt, and fine sand, respectively.

The zones of constant moisture content in Fig. 8 correspond to the continuously unfrozen zones in Fig. 6. During step one of the migration process, water from the bottom source migrated toward the frozen section in response to the temperature gradient. Although the water content in the unfrozen section changed little, a continuous supply of water was migrating through the unfrozen section and into the frozen section. The volume of water (and the total water content) in the frozen section was continually increasing, with the freezing front migrating downward. Although the total water content (including both liquid and solid-phase water) in this zone was increasing, the liquid water content was actually decreasing. TDR can monitor only the liquid water content, not the solid-phase water. Therefore, the TDR observations of water content (Fig. 8) suggest a time-dependent decline in water content in the frozen zone.

To estimate the total amount of water supplied, we used the model of moisture inflow introduced in the next section.

The Model of Moisture Inflow during the Freezing Process

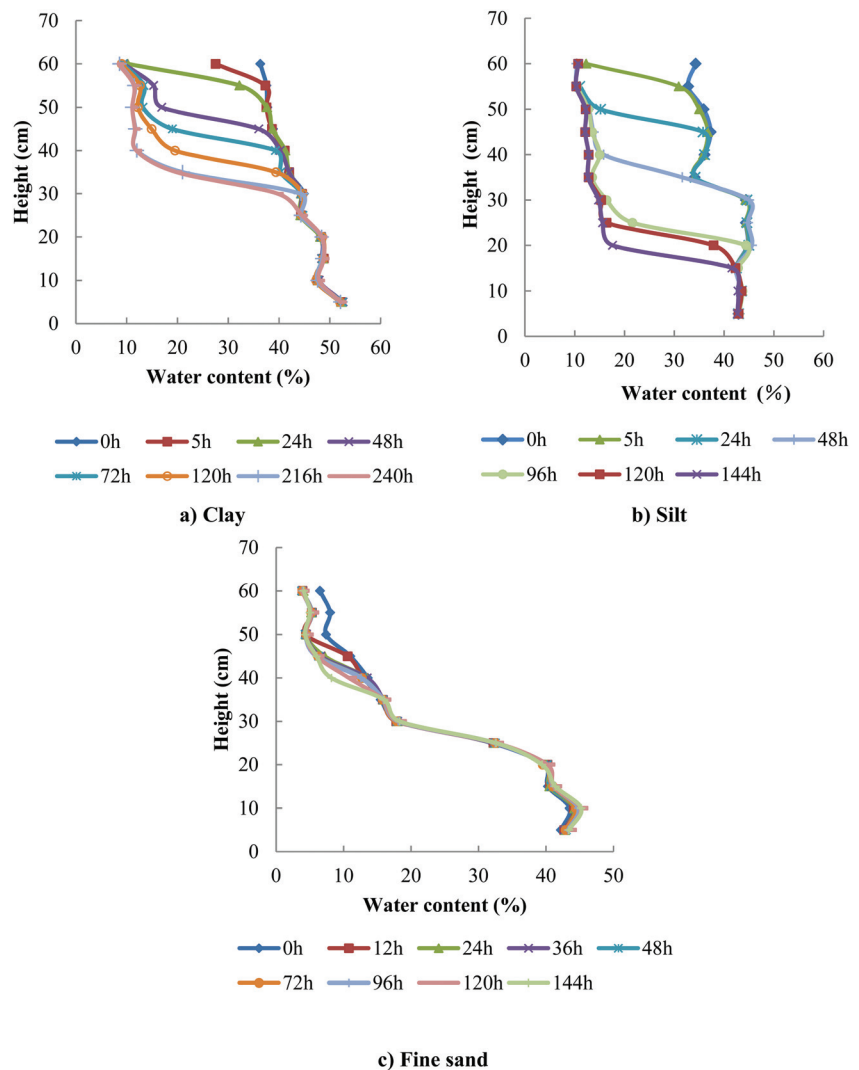
MOISTURE INFLOW VARIATION DURING THE FREEZING PROCESS

The term “moisture inflow” refers to the water flux passing the elemental area at the base of the column, expressed in units of centimeters per second.

Time variant curves were plotted (Fig. 9) for both moisture inflow and freezing rate for the three samples. With an increase in the freezing time, the moisture inflow increased, reached a peak, and underwent subsequent decline. The moisture inflow was very different in the three stages of the freezing process. In the quick frost stage, the soil was frozen quickly in place, with little moisture inflow from the bottom source. In the transition frost stage, the freezing rate began to stabilize, moisture inflow increased, and isolated (segregated) ice formations developed. In the stable frost stage, the moisture inflow reached a

FIG. 8

Liquid water content during the freezing process.



maximum rate and then began to decrease. Each of the three stages is identified in Fig. 9.

THE WATER CONTENT VARIATION FOLLOWING THE FREEZING PROCESS

The liquid water content variation curves are shown in Fig. 10 for the initial steady state condition, the final frozen state condition, and the post-freezing condition (melt) for each of the columns. This figure shows the initial distribution of moisture in each soil column prior to the application of freezing conditions from the upper boundary of the column. The final (liquid) water content in the column, as measured via TDR following the application of the freezing condition, is also displayed in this figure. Finally, the figure also shows the moisture distribution in the column following the elevation of temperatures above freezing throughout the column. The figure clearly illustrates the reduction in liquid water content that occurred in the frozen section of the column, as well as the elevated liquid water

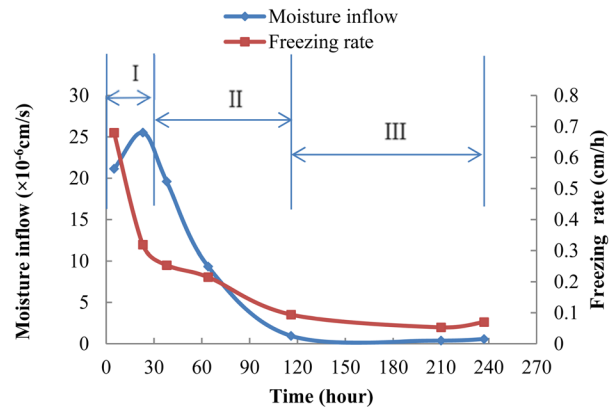
contents in the previously frozen regions after the ice was converted to liquid at the cessation of freezing, further indicating the migration of liquid water into this zone during the freezing process. A comparison of Fig. 10 with Fig. 6 reveals the correspondence between the location of the final depth of the freezing front (30 cm, 15 cm, and 30 cm for the clay, silt, and sand columns, respectively) and the depth associated with liquid water content reduction in the frozen soil columns (30 cm, 15 cm, and 30 cm for the clay, silt, and sand columns, respectively). These are the same depths discussed in the section “The Moisture Distribution in Different Stages” associated with the extent of the no-frost zone.

THE MODEL OF MOISTURE INFLOW

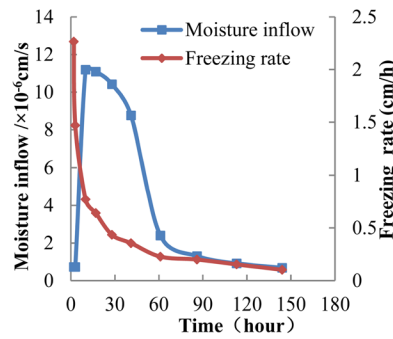
As described in the experimental results (above), the temperature reduction and induced gradient were the primary factors promoting moisture migration. The rate and volume of moisture inflow are key predictors of frost heave. Konrad and

FIG. 9

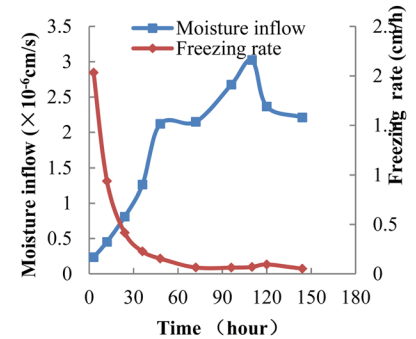
Time variant curves of moisture inflow and freezing rate for each sample.



a) Clay (I quick frost stage, II transition frost stage, and III stable frost stage)



b) Silt



c) Fine sand

Morgenstern (1981) expressed the moisture inflow V as proportional to the temperature gradient in the frozen fringe as follows:

$$(1) \quad V = (SP)(T_{\text{grad}})$$

where:

V = moisture inflow rate, cm/s,

T_{grad} = temperature gradient, °C/cm, and

SP = segregation potential, $\text{cm}^2/^\circ\text{C}/\text{s}$.

In Konrad and Morgenstern’s analysis (1981), the SP was the ratio of two measurable quantities, the moisture inflow rate and the temperature gradient across the active system for constant temperature boundary conditions, both determined at the formation of the final ice lens.

In Eq 1 SP is assumed to be a single-valued function, determined at only one point of the experiment. However, both the temperature gradient and the moisture inflow rate are variable during the experiment. If these variations are incorporated in Eq 1, it is clear that the segregation potential is not well represented by a single constant-value parameter. One unique feature

of the present research is that we have extended the use of the segregation potential concept. The revised term is *generalized* segregation potential (ψ , $\text{cm}^2/^\circ\text{C}/\text{s}$). The generalized segregation potential ψ was a time-variant function, dependent on both temperature gradient and moisture inflow rate. It was previously shown that both these parameters are related to the freezing rate, and thus ψ is also dependent on the freezing rate as shown in Fig. 11.

Although there is a clear relationship between generalized segregation potential and freezing rate, the form of that relationship is dependent on the experimental soil characteristics. Various curve-fitting techniques were evaluated to determine the functional relationship for each of the three soils in these experiments. The following are the best-fit relationships.

For clay,

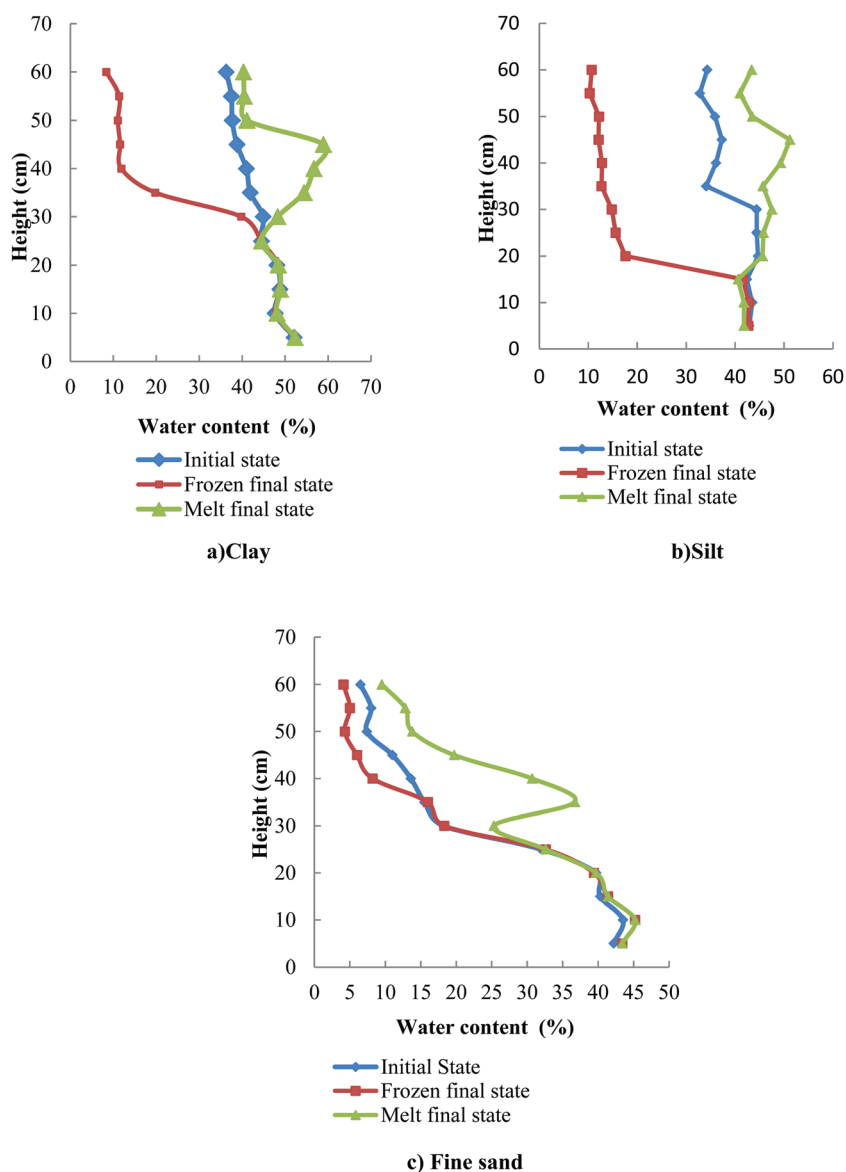
$$(2) \quad \psi = 47.771e^{-0.0069F}$$

For silt,

$$(3) \quad \psi = 45.132e^{-0.0071F}$$

FIG. 10

Liquid water content of the samples in initial, frozen, and melt states.



For fine sand,

$$(4) \quad \psi = 1.8298F^{-0.8851}$$

where:

F = freezing rate, cm/s, and

ψ = generalized segregation potential, $\text{cm}^2/^\circ\text{C}/\text{s}$.

Other terms are defined as in Eq 1.

Applying Eq 1 for this new term of generalized segregation potential, we arrive at

$$(5) \quad V = \psi T_{\text{grad}}$$

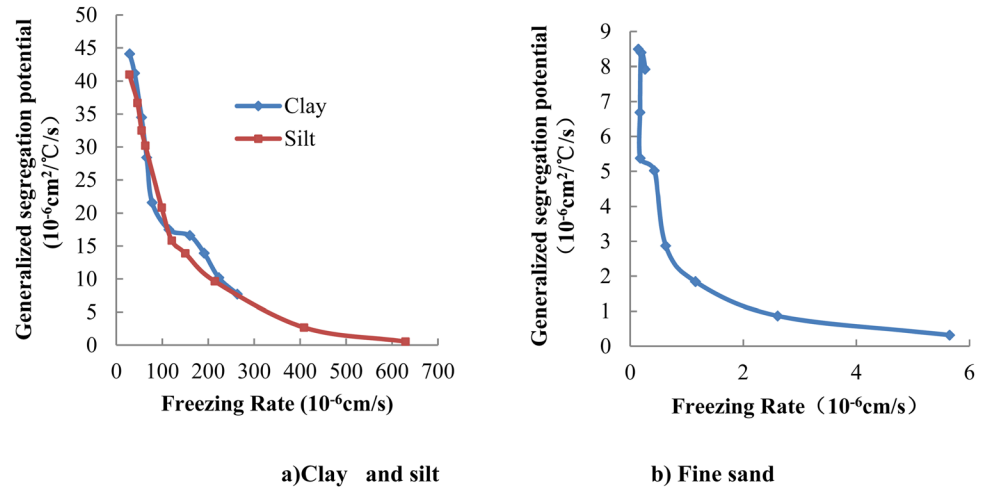
With Eqs 2 through 5, the moisture inflow can be estimated for any time during the frost progression.

VALIDATION OF THE MODEL OF MOISTURE INFLOW

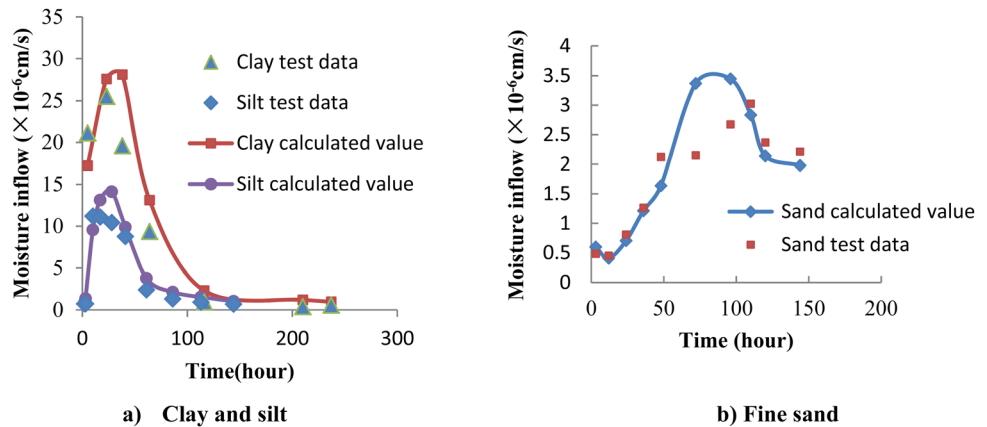
The moisture inflow predicted using Eq 5 and functional relationships of Eqs 2 through 4 for clay, silt, and fine sand were compared to the measured values of moisture inflow for this experiment (Fig. 12). The predicted values corresponded well to the measured values in the early stages of freezing. With the progression of freezing, the predicted moisture inflow exceeded the measured values. However, toward the latter stages of the freezing process, the predicted values again closely reflected the observed moisture inflow values. The maximum deviation between the measured and predicted values for the clay, silt, and sand experiments was 11.5 %, 26.0 %, and 40.0 %, respectively. However, during the early and late portions of the experiments, the average deviations were much smaller (on the order of 5 %).

FIG. 11

Generalized segregation potential as a function of freezing rate.

**FIG. 12**

Comparison between prediction and measurement of moisture inflow.



On the whole, the model was able to predict the moisture inflow with reasonable accuracy.

Conclusions

The research presented in this paper provides important insights into the development of subgrade ice layers in permafrost areas. An experimental system was constructed to monitor the initiation and progression of freezing and moisture uptake by three different soil types. The observed features of the time-variant characteristics of moisture inflow and frost penetration were used to develop a predictive model of moisture inflow. The specific conclusions of this research are the following:

1. Excavation of a region of significant highway damage along the Hoh Xil pass of Qinghai to Tibet revealed the important contribution of ice lens development to the disruptive surface damage.
2. The observations from the experimental process confirmed the presence of three distinct stages of the freezing

process: the quick frost stage, the transition frost stage, and the stable frost stage.

3. The moisture migration into the column was greatest for large temperature gradients and early periods of freezing. As freezing continued, the moisture inflow increased to a maximum value. Following this peak, the freezing rate declined and the moisture inflow decreased. By the conclusion of the experiment, a steady condition had been achieved with moisture inflow reduced to negligible values.
4. A new form of segregation potential was developed to account for the time-variant nature of the process. The new term, generalized segregation potential, was used in the development of predictive models for moisture inflow. The developed model reflects the observations reasonably well, with maximum deviations occurring during the transitional frost stage. However, during the early and late portions of the experiments, the average deviations were much smaller (on the order of 5 %). On the whole, the model was able to predict the moisture inflow with reasonable accuracy.

ACKNOWLEDGMENTS

This research was funded by the National Natural Science Foundation (50708009), Western Transportation Construction Science and Technology (2007 318 223 01-1; 2011 318 223 630), the Special Fund for Basic Scientific Research of Central Colleges, Chang'an University (CHD2010ZD003), and China Scholarship Council. The Wayne State University Department of Civil and Environmental Engineering provided office space and research facilities for the analysis of test results and preparation of the manuscript.

References

- Arenson, L. U., Azmatch, T. F., Segó, D. C., and Biggar, K. W., 2008, "A New Hypothesis on Ice Lens Formation in Frost-susceptible Soils," *Proceedings of the Ninth International Conference on Permafrost*, Fairbanks, Alaska, Institute of Northern Engineering, University of Alaska Fairbanks, Vol. 1, pp. 59–64.
- Azmatch, T. F., Arenson, L. U., Segó, D. C., and Biggar, K. W., 2008, "Measuring Ice Lens Growth and Development of Soil Strains during Frost Penetration Using Particle Image Velocimetry (GeoPIV)," *Proceedings of the Ninth International Conference on Permafrost*, Fairbanks, Alaska, Institute of Northern Engineering, University of Alaska Fairbanks, Vol. 1, pp. 89–93.
- Azmatch, T. F., Arenson, L. U., Segó, D. C., and Biggar, K. W., 2011, "Tensile Strength and Stress–Strain Behavior of Devon Silt under Frozen Fringe Conditions," *Cold Reg. Sci. Technol.*, Vol. 68, pp. 85–90.
- Bronfenbrener, L. and Bronfenbrener, R., 2010, "Modeling Frost Heave in Freezing Soils," *Cold Reg. Sci. Technol.*, Vol. 61, pp. 43–64.
- Cheng, G. D., 1981, "Unidirectional Aggregation Effect of Unfrozen Water under Seasonal Frost and Thaw Layer," *Chinese Science Bulletin*, Vol. 26, No. 23, pp. 1448–1451.
- Chou, Y. L., Sheng, Y., Wei, Z. M., and Ma, W., 2008, "Calculation of Temperature Differences between the Sunny Slopes and the Shady Slopes along Railways in Permafrost Regions on Qinghai–Tibet Plateau," *Cold Reg. Sci. Technol.*, Vol. 53, No. 3, pp. 346–354.
- Dou, M. J., Hu, C. S., and He, Z. W., 2002, "Distributing Regularities of Subgrade Diseases in Permafrost Section of the Qinghai–Tibetan Highway," *J. Glaciol. Geocryol.*, Vol. 24, No. 6, pp. 780–784.
- Harlan, R. L., 1973, "Analysis of Coupled Heated-fluid Transport in Partially Frozen Soil," *Water Resour. Res.*, Vol. 9, No. 5, pp. 1314–1323.
- Jin, L., Wang, S. J., and Dong, Y. H., 2012, "Study on the Height Effect of Highway Embankments in Permafrost Regions," *Cold Reg. Sci. Technol.*, Vol. 83–84, pp. 122–130.
- Konrad, J. M. and Duquennoi, C., 1993, "A Model for Water Transport and Ice Lensing in Freezing Soils," *Water Resour. Res.*, Vol. 29, No. 9, pp. 3109–3124.
- Konrad, J. M. and Morgenstern, N., 1981, "The Segregation Potential of a Freezing Soil," *Can. Geotech. J.*, Vol. 18, No. 4, pp. 482–491.
- Lei, Z. D., Yang, S. X., and Xie, S. C., 1988, *Soil Water Dynamics*, Tsinghua University Press, Beijing, pp. 123–125.
- Liu, Y. Z., Wu, Q. B., Zhang, J. M., and Sheng, Y., 2002, "Deformation of Highway Roadbed in Permafrost Regions of the Tibetan Plateau," *J. Glaciol. Geocryol.*, Vol. 24, No. 1, pp. 10–15.
- Mao, X. S., Hou, Z. J., Wang, W. N., and Lu, L., 2010, "Formation Mechanism and Numerical Simulation of Longitudinal Crack in Wetland Section of Qinghai–Tibet Highway," *Chinese J. Rock Mech. Eng.*, Vol. 29, No. 9, pp. 1915–1921.
- Miao, T. D., Guo, L., Niu, Y. H., and Zhang, C. Q., 1999, "The Model of Mixture Theory for Water–Heat Transition in Freezing Soil," *Science in China (Series D)*, Vol. 29, No. 1, pp. 8–14.
- Pei, J. Z., Dou, M. J., Hu, C. S., and Wang, B. G., 2006, "Forming Mechanism of Embankment Longitudinal Cracks in Permafrost Regions," *J. Glaciol. Geocryol.*, Vol. 28, No. 1, pp. 116–121.
- Professional Standards Compilation Group of People's Republic of China, 2007, *Regulations for Highway Soil Engineering Test (JTGE40-2007)*, China Communications Press, Beijing, pp. 36–38.
- Taylor, G. S. and Luthin, J. N., 1978, "A Model for Coupled Heat and Moisture Transfer during Soil Freezing," *Can. Geotech. J.*, Vol. 15, pp. 548–555.
- Tezera, F. A., 2012, "New Ice Lens Initiation Condition for Frost Heave in Fine-grained Soils," *Cold Reg. Sci. Technol.*, Vol. 82, pp. 8–13.
- Wang, T. H., Li, N., and Xie, D. Y., 2004, "Gravitational Potential, Matrix Suction and Thermal Potential of Unsaturated Loess Soil," *Chinese J. Geotech. Eng.*, Vol. 26, No. 5, pp. 715–718.
- Wen, Z., Sheng, Y., Ma, W., and Wu, Q. B., 2009, "Ground Temperature and Deformation Laws of Highway Embankments in Degenerative Permafrost Regions," *Chinese J. Rock Mech. Eng.*, Vol. 28, No. 7, pp. 1477–1483.
- Xu, X. Z., Tao, Z. X., and Fu, S. L., 1981, "The Thermal Properties of Typical Thawing and Freezing Soils," *The Collected papers of the Lanzhou Institute of Glaciology and Geocryology*, Chinese Academy of Science, pp. 55–71.
- Xu, X. Z., Wang, J. C., and Zhang, L. X., 2001, *The Physics in Freezing Soil*, Science Press, Beijing, pp. 178–180.
- Zhang, X. F., Xin, D. G., Zhang, D. Q., and Wang, X. R., 2004, "Water Migration and Variation in the Subgrade Soils of Expressway in Seasonally Frozen Ground Regions," *J. Glaciol. Geocryol.*, Vol. 26, No. 4, pp. 454–460.